

# UWB-MIMO DGS loaded patch antenna with low profile for millimeter-wave applications

Ajay Kumar Dwivedi<sup>1</sup>, Nagesh Kallollu Narayaswamy<sup>1</sup>,  
Vivek Singh<sup>2</sup>, Mallanna Sidramappa Darmanar<sup>2</sup>

A multiple-input multiple-output (MIMO) antenna with a defective ground surface (DGS) is proposed for next-generation millimeter-wave communication. The designed antenna consists of a pair of mushroom shape radiating units with two square ring-loaded defected common ground plane. The antenna is printed on duroid-5880 high-frequency laminates (loss tangent 0.0009, relative permittivity 2.2). Significant bandwidth ranges from 31.6 GHz to 48.8 GHz (impedance bandwidth of 43.17%) is obtained during the investigation of the antenna. The introduced MIMO antenna exhibits a low mutual coupling ( $|S_{21}|, |S_{12}| < -20$ ) dB with the incorporation of DGS. The antenna performance parameters defined as return loss, radiation pattern, gain, the radiation efficiency is examined. Many diversity parameters are also discussed in terms of mutual coupling, envelop correlation coefficient ( $ECC < 0.002$ ), diversity gain ( $DG > 9.995$ ), and channel capacity loss ( $CCL < 0.3$  bits/sec/Hz) across the ultra-wide band (UWB) frequencies. Simulated results are verified by the measured results, and good agreement is observed between them. These distinguishable attributes with the simple configuration model the propound MIMO antenna suitable for millimeter-wave applications.

**Key words:** square ring, MIMO antenna, defected ground surface, envelope correlation coefficient, diversity gain, UWB, patch antenna

## 1 Introduction

In the modern communication system, the transmitted data and voice signals are affected by multipath fading phenomena during transmission. To overcome the fading issues, three techniques are evolved by the researchers during studies of the higher generation of communication system, (i) – orthogonal frequency division multiplexing (OFDM), (ii) – adaptive modulation techniques, (iii) – multiple-input multiple-output transceiver units, [1]. In this work multiple-input, multiple-output (MIMO) antenna system is considered and modelled. MIMO an-

tenna system comprises of the number of transmitting and receiving antennas to provide multiple channel paths for data transmission and thus provide better channel capacity with limited power requirements. The requirement for the designing of the MIMO antenna is to mitigate the mutual coupling between the different antenna units present in a single entity. For the appropriate operation of the MIMO antenna, the isolation factor should be less than  $-15$  dB. Since the last decades, the patch antenna-based UWB-MIMO technologies have attracted the attention of many researchers due to their higher data rates capabilities and ease of fabrication. Several poten-

**Table 1.** Dimensions of the suggested uwb-mimo antenna

Ref.	Area (mm <sup>2</sup> )	Bandwidth (GHz)	Isolation (dB)	Peak gain (dBi)	Radiation efficiency	ECC
4	126 × 126	24 – 36	> 20	7.8	> 70	< 0.005
5	30 × 35	25.5 – 29.6	> 17	8.3	> 80	< 0.01
6	80 × 80	23 – 40	> 20	11.45	> 70	< 0.0012
7	30 × 30	27 – 29	> 29	6.1	> 92	< 0.16
8	110 × 75	26.3 – 30	> 21	9.53	> 73	< 0.2
This work	44 × 22	31.6 – 48.8	> 20	10.23	> 93	< 0.002

<sup>1</sup> Department of Electronics and Communication, Nitte Meenakshi Institute of Technology, Bengaluru, India, er.ajaydwivedi@gmail.com, nageshlakmaya@gmail.com, <sup>2</sup> Department of Electronics and Communication, Nagarjuna College of Engineering and Technology Bengaluru, Karnataka, India, vivek.10singh@gmail.com, mallanna.sugur@gmail.com

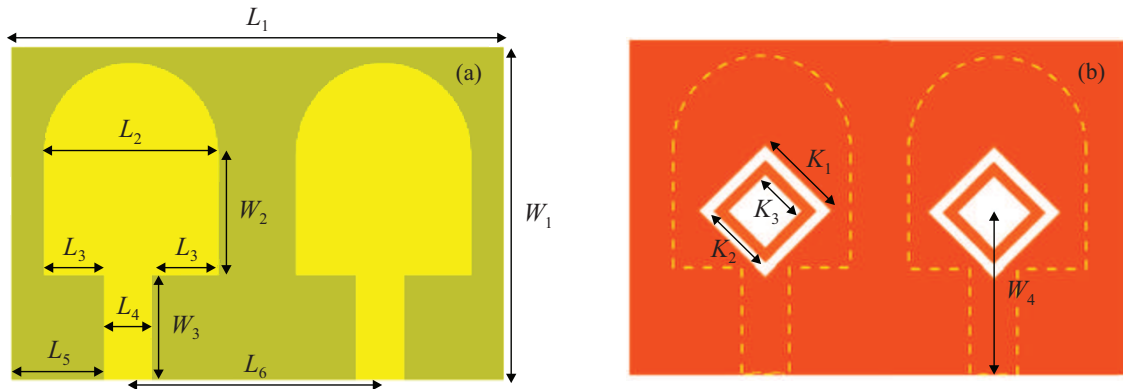


Fig. 1. Geometrical configuration of the suggested antenna: (a) – top view, (b) – bottom view

tial bands are investigated by the researcher in millimeter-wave spectra such as the 28 GHz (27.5–29.5 GHz) band, 38 GHz (3640 GHz) band, the 60 GHz (5764 GHz) band, and the E-band (7176 and 8186 GHz), [2]. Any specific regulations for the wireless system and technologies are not been clearly defined for the mm-wave communication band till now. However, scientists and researchers around the globe are working on two bands (28 GHz and 38 GHz sub-GHz) of 5G communications under the mm-wave frequency range. These two bands are chosen as the prominent bands for 5G communication because the effect of rain attenuation and atmospheric disturbance are feeble on the aforementioned frequencies, [3]. Many techniques have been projected by the researchers to obtain the UWB-MIMO patch antennas for millimeter-wave applications, [4-8]. Many techniques have been suggested by the researchers to improve isolation, [9-14]. However, the incorporation of various irregular terrains for isolation enhancement will increase the antenna footprint and hence complexity. A  $9 \times 9$  MIMO antenna is developed for the operating band of 24 GHz to 39 GHz [4]. In [4], isolation more than -20 dB is achieved in absence of any decoupling unit. In [5] a 4-port multiple-input-multiple-output (MIMO) antenna array is presented in the mm-wave range. To improve the antenna's radiation properties, the array components are rectangular-shaped slotted patch antennas, while the ground plane is defective with rectangular, circular, and zigzag-shaped slotted structures. For 5G communication in the millimeter-wave range, a compact tree form planar quad element Multiple Input Multiple Output (MIMO) antenna with a broad bandwidth is suggested [6]. To accomplish the broad bandwidth response, the suggested design includes four distinct arcs in the radiating element. A 28 GHz MIMO antenna is presented in [15] in which infinity-shaped shell with circular circles surrounding it. In [8] MIMO antenna for mm wave applications is proposed. Goals of this work are to show an integrated antenna solution for long term evolution (LTE) and millimeter wave (mm-wave) 5G wireless services. Both an LTE and 5G configuration are included in the suggested design, which includes both an antenna and a ground plane that has irregularly shaped holes.

Table 1 shows a comparison of the proposed antenna with other previously published MIMO antennas for mm-wave applications. When compared to other published antennas, the suggested UWB-MIMO antenna has a broader impedance bandwidth, higher gain, radiation efficiency with outstanding isolation between antenna units, and diversity performance.

In this communication, a compact UWB-MIMO patch antenna for mm-wave scenarios is presented. The suggested antenna is modelled, simulated, and optimized using the 3-D electromagnetic high-frequency structure simulator (HFSS-18), and the fabricated prototype is experimentally verified. Between the simulated and measured findings, a healthy agreement is obtained. Because of its high diversity gain, low envelope correlation coefficient (ECC), and limited mutual coupling between the inter-element antenna units across the full UWB frequency range, the proposed antenna is a good fit for MIMO millimeter-wave applications.

Table 2. Dimensions of the suggested UWB-MIMO antenna

Parameters	Value (mm)	Parameters	Value (mm)
L1	44	W2	7
L2	12	W3	5
L3	4.5	W4	8
L4	3	K1	5.65
L5	9.5	K2	4.24
L6	22	K3	2.82
W1	22	H	1.6

## 2 Antenna configuration

The geometrical arrangement of the suggested UWB-MIMO antenna is depicted in Fig. 1. The designed antenna is printed on commercially available high-frequency

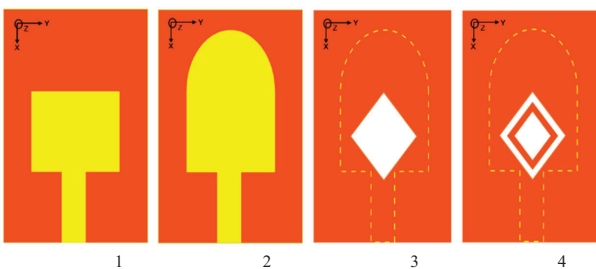
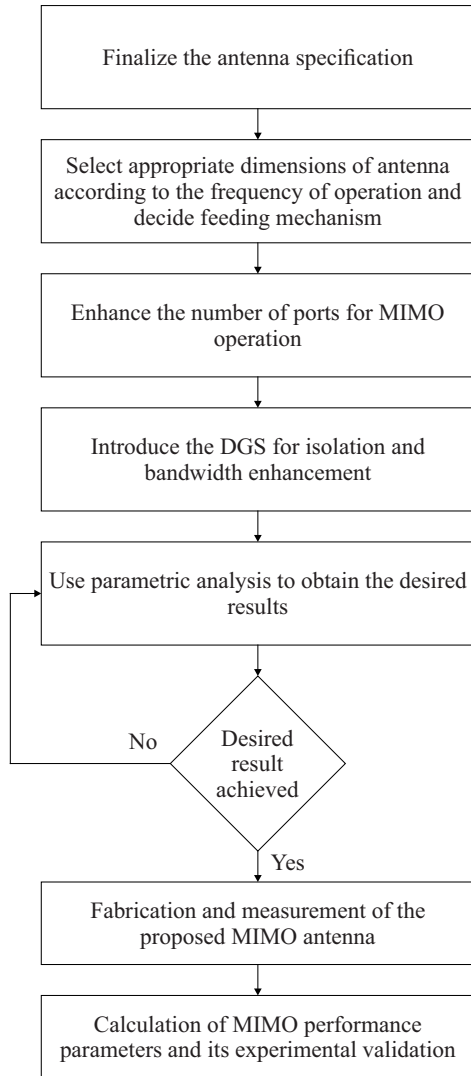


Fig. 2. Design steps to obtain the suggested antenna

laminates duroid 5880 substrates with relative permittivity ( $\epsilon_r = 2.2$ ) and loss tangent ( $\tan\delta = .0009$ ) of a thickness of 1.6 mm. The upper conducting portion comprises feed lines, and two radiating units of mushroom shape, and the lower portion of substrate consist of a square ring-loaded defected ground plane. Here, a single antenna unit is obtained by adjoining the rectangle of the dimension of  $L_2 \times W_2$  with a semi-circle of diameter  $L_2$  and coplanar waveguide of length  $W_3$  and thickness of  $L_4$ . The second antenna unit is a mirror image of the first antenna unit, formed at the same surface at the optimized distance of

$L_6$  from unit 1. Ultra-wideband is obtained by incorporating the square ring of an optimized dimension on the ground.

Table 2 lists the optimal dimensions of the proposed MIMO antenna. Each of the antenna units is fed with  $50\Omega$  CPW to obtain the perfect impedance matching.

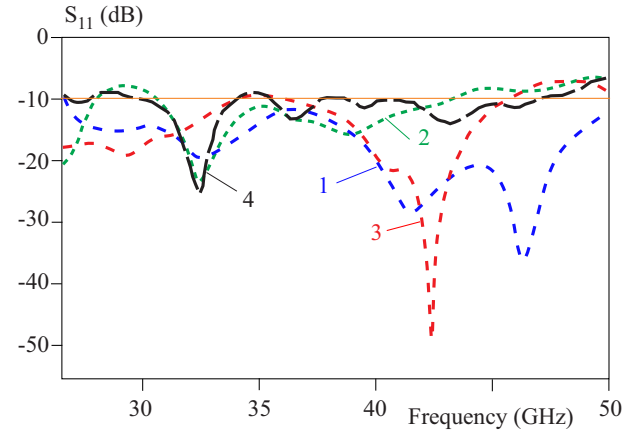


Fig. 3.  $|S_{11}|$  variations for antenna 1 to 4 configurations

In order to show the stepwise growth, a flow chart is included.

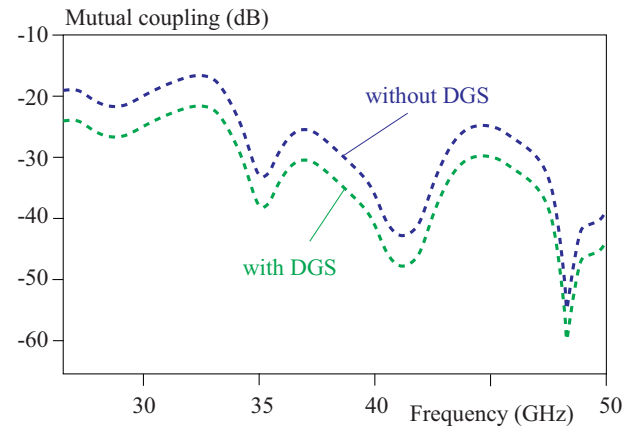
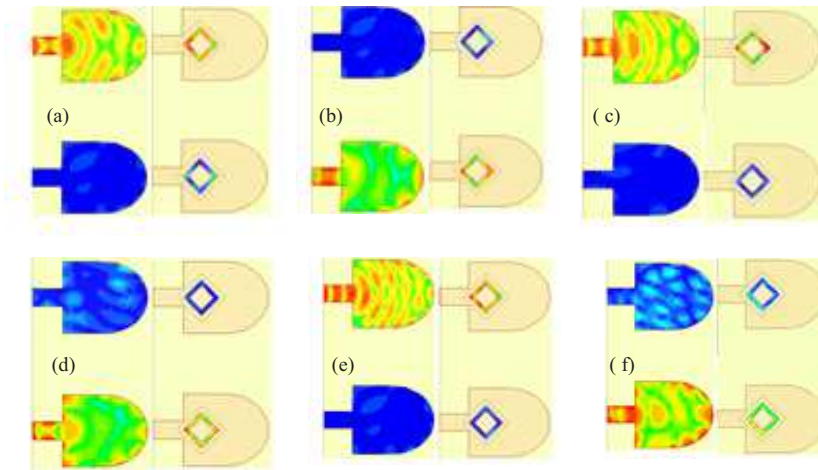


Fig. 4. Effect of DGS on the mutual coupling between the antenna units for the suggested antenna

### 3 Antenna analysis

Figure 2 represents the evolution stage to achieve the single antenna element of the suggested MIMO antenna. Figure 3 represents the variation in the  $|S_{11}|$  characteristic of these stages. In the primary phase, CPW fed rectangular shape antenna 1 is designed to obtain the UWB characteristics in the millimeter-wave range, which further converted into antenna 2 by adjoining a semi-circular patch of diameter  $L_2$  on the top of the rectangular patch. From the introspection of Figure 3, conversion from antenna 1 to antenna 2 increases the impedance bandwidth,



**Fig. 5.** Surface current distribution of suggested UWB-MIMO antenna at: (a) – 35 GHz at port 1, (b) – 35 GHz at port 2, (c) – 38.4 GHz at port 1, (d) – 38.4 GHz at port 2, (e) – 44.2 GHz at port 1, and (f) – 44.2 GHz at port 2

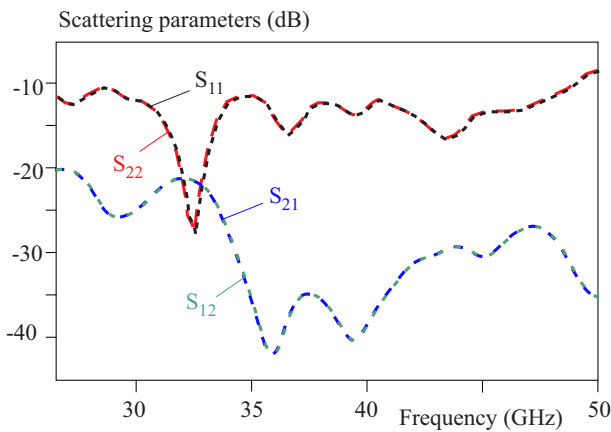


**Fig. 6.** The simulated scattering parameters for the suggested MIMO antenna

but still, it shows the dual-band behavior. Now for the enhancement of bandwidth, a square shape slot is incorporated on the ground plane depicted in antenna 3. Finally, a square ring is introduced on the ground within the slot

to obtain the suggested configuration, *ie* antenna 4 with optimum ultra-wide bandwidth. From the observation of figure 3, antenna 4 has maximum impedance bandwidth from 31.6 GHz to 48.8 GHz. In the subsequent design, the orientation and positioning of the slot and rectangular ring made on the ground also play a crucial role in achieving the ultra-wide bandwidth characteristics.

The effects of a defective ground surface on the mutual coupling between antenna units are shown in Fig. 4. The mutual coupling between the antenna units is (–15 dB) prior to the induction of DGS. After the incorporation of DGS, the value of mutual coupling further mitigates to (< –20 dB) and restrains the surface wave on the ground plane to couple to another antenna element.

Figure 5 depicts the surface current distribution on the patch and DGS to better understand the isolation phenomenon for the proposed MIMO antenna. At three resonant frequencies of 35 GHz, 38.4 GHz, and 44.2 GHz, the current distribution for the intended antenna is illustrated. From the inspection of Figure 5, the maximum current distribution is concentrated on port 1 when

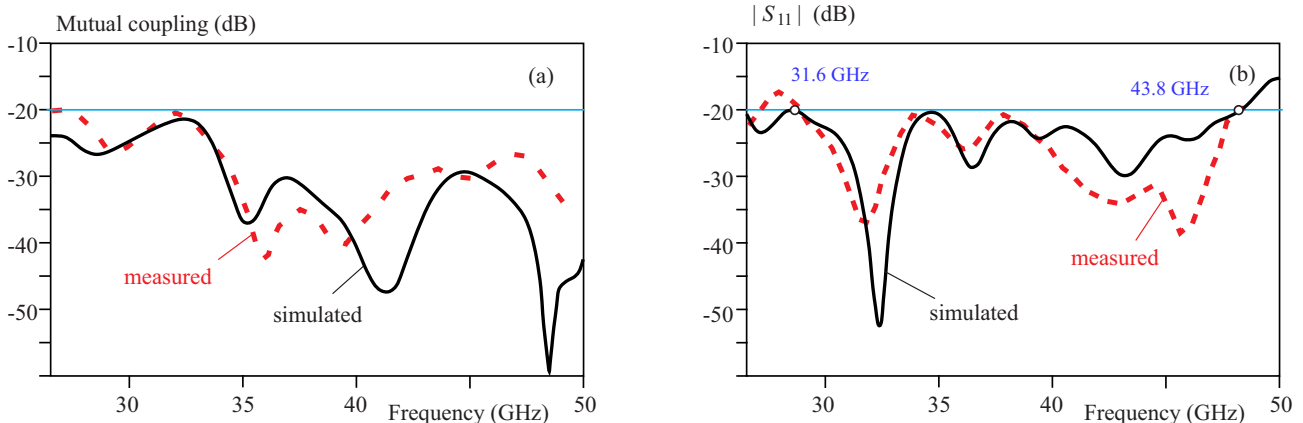


**Fig. 7.** Measured and simulated: (a) – reflection coefficient, (b) – mutual coupling of designed antenna

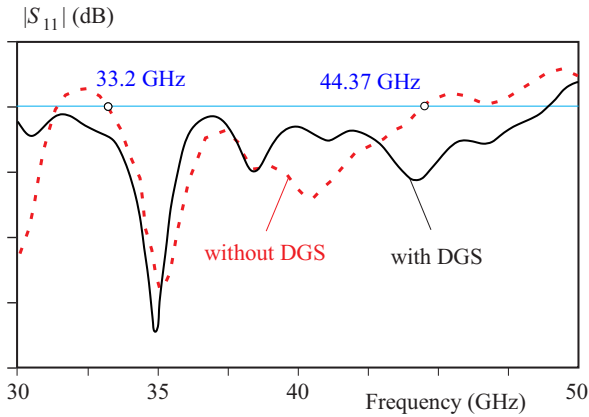


Fig. 8. Variation in  $|S_{11}|$  plot with and without defected ground surface for suggested UWB-MIMO antenna.

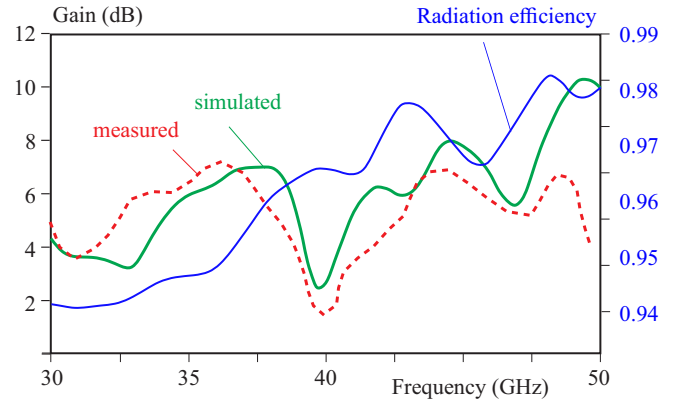


Fig. 9. Simulated and measured Gain and Radiation efficiency of the suggested UWB-MIMO antenna

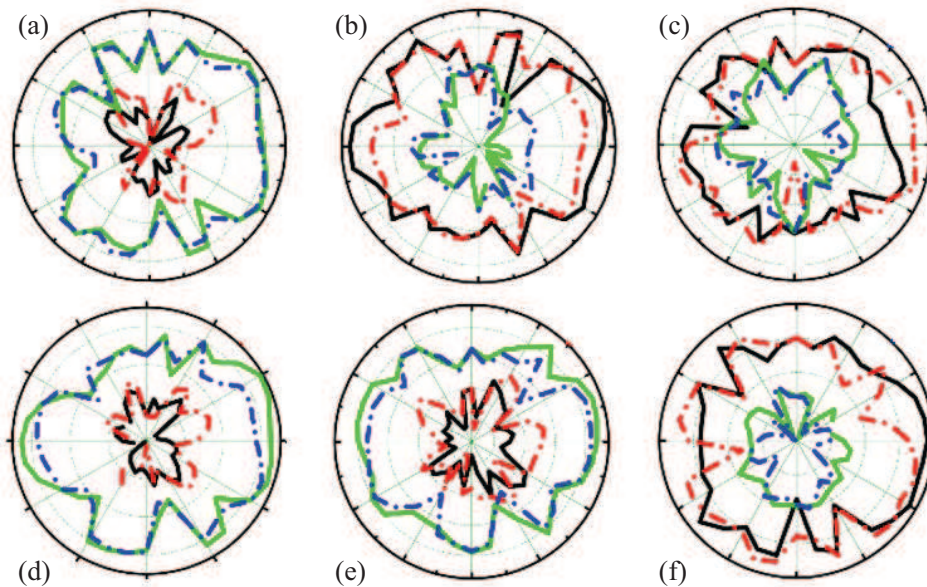


Fig. 10. Radiation pattern of the suggested UWB-MIMO antenna at: (a) – 35 GHz in E-plane, (b) – 35 GHz in H-plane, (c) – 38.4 GHz in E-plane, (d) – 38.4 GHz in H-plane, (e) – 44.2 GHz in E-plane, and (f) – 44.2 GHz in H-plane.

it is exciting, and similar behavior is observed when port 2 is sourced. The basic requirements of isolation between the ports can be easily understood by the current distribution phenomena. DGS cancels out the fields between adjacent antenna units, effectively stopping the current passage between them. Hence the enhancement in terms of isolation is achieved between the antenna units.

#### 4 Results and discussion of MIMO antenna

The 2-port MIMO antenna is extended from the single-port antenna unit. Fig. 6 shows the simulated scattering parameters ( $|S_{11}|$ ,  $|S_{22}|$ ,  $|S_{12}|$ , and  $|S_{21}|$ ) for the proposed MIMO antenna, while Fig. 7 shows the measured counterparts of the simulated outcome. The suggested antenna, as shown in Fig. 6 and 7, operates throughout an ultra-wideband of 31.6 GHz to 48.8 GHz, with isolation better

than 20 dB throughout the frequency range. The simulated and measured findings exhibited inconsistencies at higher frequencies due to a lack of measurement precision and the influence of manufacturing tolerance.

Figure 8 depicts the  $|S_{11}|$  plot for the proposed UWB-MIMO antenna with and without DGS. The incorporation of DGS increases the impedance bandwidth from 33.2 – 44.37 GHz to 31.6 – 48.8 GHz.

The measured and simulated gain and simulated radiation efficiency of the suggested antenna are depicted in Fig. 9. The maximum gain is 10.23 dB, and the overall radiation efficiency is better than 93%. The perturbation in the gain plot is observed because, at the millimeter-wave frequency, the atmospheric disturbance becomes prominent. However, in the suggested configuration, the gain has significant values for the whole bandwidth.

Figure 10 shows simulated and measured co and cross-polarization plots in the  $XZ$  and  $YZ$  planes for three

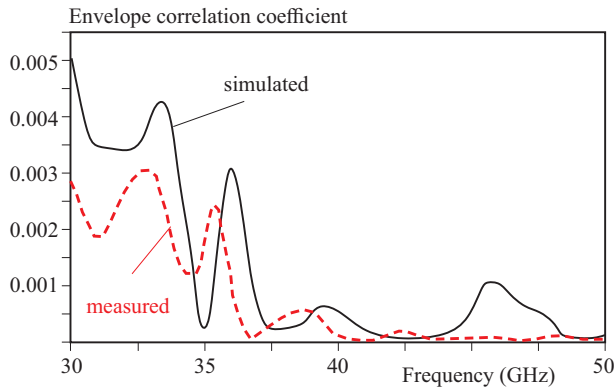


**Fig. 11.** ECC comparison between the simulated and measured value of the 2 port MIMO antenna

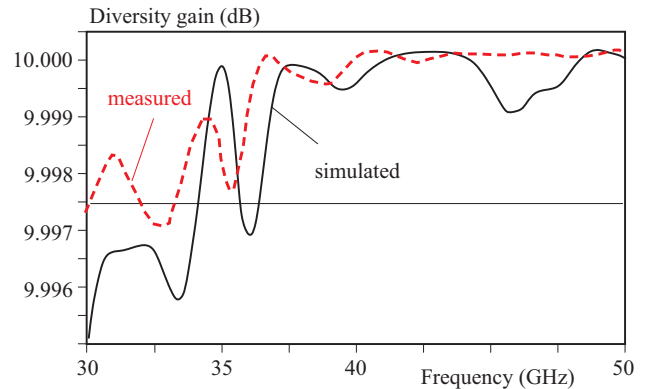


**Fig. 12.** Simulated and measured value of diversity gain of the MIMO antenna

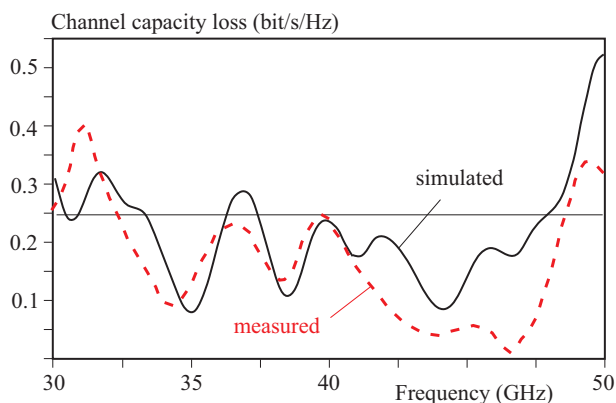


**Fig. 13.** Simulated and measured variation curve of CCL of the suggested MIMO antenna

resonant frequencies of 35 GHz, 38.4 GHz, and 44.2 GHz. The difference between the co-polarized and cross-polarized levels is found to be considerable. The radiation pattern is created by stimulating one port and stopping the other with a 50 matched load. The measurements and simulations' results are found to be incoherent.

### 5 MIMO antenna diversity performances

The correlation coefficient function  $\rho$ , indicates how isolated or correlated the communication channels are from one another. Among the primary factors for calculating diversity in MIMO antennas, the envelope correlation coefficient is one of the most important, since it reveals in great detail how the different ports are related to each other. The ECC is formulated in two ways: (i) – by using  $(\rho)$  scattering parameter (ii) – by using a 3-dimensional far-field radiation pattern. To achieve the best results, the upper limit of ECC should be  $< 0.5$  [1] [16]. When the antenna radiation efficiency is greater than 90%, the scattering parameters approach for calculating ECC should be employed. The following equation can be

used to compute the ECC for a two-unit MIMO system

$$|\rho_{nm}|^2 = \rho_{enm} = \frac{|S_{nn}^* S_{nm} + S_{mn}^* S_{mm}|^2}{\left( (1 - |S_{nm}|^2 - |S_{mm}|^2) (1 - |S_{mm}|^2 - |S_{nn}|^2) \right)}, \quad (1)$$

where  $\rho_{nm}$  and  $\rho_{enm}$  is the correlation coefficient and envelope correlation coefficient respectively and  $S_{nm}$ ,  $S_{mn}$  shows the return loss and mutual coupling scattering factors between the antenna's ports. Figure 11 shows the variations in the simulated and measured value of ECC. It can be seen from Figure 11 that the resulting value of ECC is  $(< 0.002)$ , which is significantly better than the optimal value of (0.5), indicating that the ports on the antenna element have a better correlation.

The alternative approach for computing ECC is more efficient since it takes into account the details of the 3D distant radiated field, despite the apparent port coupling. The 3D far radiation pattern  $E_j(\theta, \phi)$  is seen here when power is applied to the  $i$  th and  $j$  th ports at the same time, and  $\Omega$  is the solid angle. To calculate the ECC we use, [16]

$$\rho_e = \frac{\left| \iint_{4\pi} E_i(\theta, \phi) E_j(\theta, \phi) d\Omega \right|^2}{\iint_{4\pi} |E_i(\theta, \phi)|^2 d\Omega \iint_{4\pi} |E_j(\theta, \phi)|^2 d\Omega}. \quad (2)$$

This is defensible when the isotropic environment is considered. When the transmitter gets data from multiple channels, diversity is achieved. When transmissions are significantly uncorrelated, the combined signals at the receiver end give an increase in SNR levels, resulting in increased signal reception [14] [17]. The DG is computed by

$$DG = \sqrt{1 - ECC}. \quad (3)$$

The correlation coefficient is related to the diversity gain. The larger the diversity gain, the lower the coefficient

value. The comparison of simulated and measured values from Fig. 12 confirms that the suggested antenna has a better diversity function in the operating range.

Suggested antenna CCL variation is shown in Fig. 13. CCL gives the information regarding the maximum quantity of data that may be sent continuously in the communication channel without any loss of data occurred. It can be calculated by the use of the following equations, [1].

$$\begin{aligned}
 CCL &= -\log \det \begin{bmatrix} a_{11} & a_{12} \\ a_{21} & a_{22} \end{bmatrix} \\
 a_{11} &= 1 - (|S_{11}|^2 + |S_{12}|^2) \\
 a_{22} &= 1 - (|S_{22}|^2 + |S_{21}|^2) \\
 a_{12} &= -(S_{11}^* S_{12} + S_{21}^* S_{12}) \\
 a_{21} &= -(S_{11}^* S_{12} + S_{21}^* S_{12}) \\
 a_{21} &= -(S_{22}^* S_{21} + S_{12}^* S_{21}) .
 \end{aligned} \tag{4}$$

(4) For a better diversity function, the practical, acceptable range of CCL ( $< 0.4$  bits/sec/Hz). From Fig. 13, it is found the suggested antenna has the CCL level ( $< 0.3$  bits/sec/Hz), which confirms the improved diversity function.

## 6 Conclusion

An ultra-wideband defected ground surface loaded  $1 \times 2$  MIMO antenna is presented and discussed. Enormous potential bandwidth of 17.2 GHz ranges from 31.6 – 48.8 GHz is obtained for mm-wave applications. The use of DGS not only improves bandwidth, but it also mitigates mutual coupling between antenna parts significantly. The effectiveness of the MIMO antenna is verified by calculating various parameters in terms of ECC, DG, and CCL, with the results indicating that the suggested antenna is adequate for MIMO next-generation wireless communication within the specified bands. Recently published studies often offer comparative figures to substantiate the originality of the suggested antenna design.

## REFERENCES

- [1] M. S. Sharawi, *Printed MIMO Antenna Engineering*, Boston, London: Artech House Inc., 2014.
- [2] A. A. R. Saad and H. A. Mohamed, "Printed millimeter-wave MIMO-based slot antenna arrays for 5G networks, *AEU - Int. J. Electron. Commun.*, vol. 99, pp. 5969, Feb. 2019, doi: 10.1016/j.aeue.2018.11.029.
- [3] T. S. Rappaport *et al*, "Millimeter Wave Mobile Communications for 5G Cellular: It Will Work!, *IEEE Access*, vol. 1, pp. 335349, 2013, doi: 10.1109/ACCESS.2013.2260813.
- [4] F. Wang, Z. Duan, X. Wang, Q. Zhou, and Y. Gong, "High Isolation Millimeter-Wave Wideband MIMO Antenna for 5G Communication, *Int. J. Antennas Propag.*, vol. 2019, pp. 112, May 2019, doi: 10.1155/2019/4283010.
- [5] M. Rahman *et al*, "Integrated LTE and millimeter-wave 5g mimo antenna system for 4g/5g wireless terminals, *Sensors (Switzerland)*, vol. 20, no. 14, pp. 120, 2020, doi: 10.3390/s20143926.
- [6] D. A. Sehrai *et al*, "A Novel High Gain Wideband MIMO Antenna for 5G Millimeter Wave Applications, *Electronics*, vol. 9, no. 6, pp. 1031, Jun. 2020, doi: 10.3390/electronics9061031.
- [7] M. M. Kamal *et al*, "Infinity Shell Shaped MIMO Antenna Array for mm-Wave 5G Applications, *Electronics*, vol. 10, no. 2, pp. 165, Jan. 2021, doi: 10.3390/electronics10020165.
- [8] M. Khalid *et al*, "4-Port MIMO Antenna with Defected Ground Structure for 5G Millimeter Wave Applications, *Electronics*, vol. 9, no. 1, pp. 71, Jan. 2020, doi: 10.3390/electronics9010071.
- [9] Z. Li, Z. Du, M. Takahashi, K. Saito, and K. Ito, "Reducing Mutual Coupling of MIMO Antennas With Parasitic Elements for Mobile Terminals, *IEEE Trans. Antennas Propag.*, vol. 60, no. 2, pp. 473481, Feb. 2012, doi: 10.1109/TAP.2011.2173432.
- [10] S. D. Assimonis, T. V. Yioultis, and C. S. Antonopoulos, "Design and Optimization of Uniplanar EBG Structures for Low Profile Antenna Applications and Mutual Coupling Reduction, *IEEE Trans. Antennas Propag.*, vol. 60, no. 10, pp. 49444949, Oct. 2012, doi: 10.1109/TAP.2012.2210178.
- [11] Y. Lee, D. Ga, and J. Choi, "Design of a MIMO Antenna with Improved Isolation Using MNG Metamaterial, *Int. J. Antennas Propag.*, vol. 2012, pp. 17, 2012, doi: 10.1155/2012/864306.
- [12] N. K. Kiem, H. N. B. Phuong, Q. N. Hieu, and D. N. Chien, "A Novel Metamaterial MIMO Antenna with High Isolation for WLAN Applications, *Int. J. Antennas Propag.*, vol. 2015, pp. 19, 2015, doi: 10.1155/2015/851904.
- [13] J. Liu, K. P. Esselle, S. G. Hay, Z. Sun, and S. Zhong, "A Compact Super-Wideband Antenna Pair With Polarization Diversity, *IEEE Antennas Wirel. Propag. Lett.*, vol. 12, pp. 14721475, 2013, doi: 10.1109/LAWP.2013.2287500.
- [14] A. K. Dwivedi, A. Sharma, A. K. Singh, and V. Singh, "Quad-port ring dielectric resonator based MIMO radiator with polarization and space diversity, *Microw. Opt. Technol. Lett.*, p. mop.32329, Feb. 2020, doi: 10.1002/mop.32329.
- [15] S. Gupta, Z. Briqech, A. R. Sebak, and T. Ahmed Denidni, "Mutual-Coupling Reduction Using Metasurface Corrugations for 28 GHz MIMO Applications, *IEEE Antennas Wirel. Propag. Lett.*, vol. 16, pp. 27632766, 2017, doi: 10.1109/LAWP.2017.2745050.
- [16] A. K. Dwivedi, A. Sharma, A. K. Singh, and V. Singh, "Metamaterial inspired dielectric resonator MIMO antenna for isolation enhancement and linear to circular polarization of waves, *Measurement*, vol. 182, pp. 109681, Sep. 2021, doi: 10.1016/j.measurement.2021.109681.
- [17] M. S. Sharawi, *Printed MIMO Antenna Engineering*, Boston, London: Artech House Inc., 2014.

Received 25 November 2021

**Ajay Kumar Dwivedi** is working as an Associate Professor in the Department of Electronics & Communication Engineering, Nagarjuna College of Engineering & Technology, Bangalore, India. He has Completed his PhD from the Department of Electronics & Communication Engineering, Indian Institute of Technology Allahabad, Prayagraj, UP (India) in 2021. In 2015 he received his M Tech Degree in wireless communication Engineering from the Sam Higginbottom University of Agriculture, Technology and Sciences, Deemed University, Allahabad, India. Completed B Tech in Electronics and Communication Engineering from the Uttar Pradesh Technical University, Lucknow, India, in 2010. He has worked as an Assistant Professor at Shambhunath Institute of Engineering and Technology, Prayagraj (UP), India, with six years of teaching experience. He has authored or co-authored more than 50 research papers in international/national journal/conference proceedings. His research interests include RF and microwave, microstrip patch antennas, wireless communication, antenna theory, Dielectric resonator antenna, MIMO and metamaterial-based dielectric resonator antenna. He is

a reviewer of many international/national journal/conference proceedings like IEEE Transactions on Vehicular Technology, Wireless Personal Communications, International Journal of Circuit Theory and Applications and Computer Networks.

**Nagesh Kallollu Narayaswamy** is working as a Professor and Head of the Department in Electronics & Communication Engineering, Nagarjuna College of Engineering & Technology, Bengaluru, India. He has completed his PhD from Jawaharlal Nehru Technological University Anantapur (JNTUA) Anantapur- AP, India in 2016. In 2007 he received his M Tech Degree in Digital electronics and communication from Nitte Mahalinga Adyanthaya Memorial Institute of Technology (NMAMIT) Mangalore, VTU, Karnataka, India. Completed BE in Electronics and Communication Engineering from Siddganga Institute of Technology (SIT) - Tumkur. VTU, Karnataka, India in 2005. He has 15 years of teaching experience to UG and PG students. He has authored or co-authored more than 35 research papers in international journal/conference proceedings. His research interests include Wireless communication, Communication system, IoT, and Antennas. He is a reviewer of many international journal/conference proceedings.

**Vivek Singh** was born in Allahabad district of UP in 1987. He obtained his B Tech Degree in electronics and communication engineering from Uttar Pradesh Technical University in 2009 and M Tech Degree in electronics engineering from the University of Allahabad in 2012. He obtained his D Phil degree in 2019 from the University of Allahabad. Currently, working as an Associate Professor in the Department of Electronics & Communication Engineering, Nagarjuna College of Engineering & Technology, Bangalore, India. His research interests include modeling and simulation of RF devices and circuits and their applications.

**Mallanna Sidramappa Darmanar** is currently working as Assistant Professor in Nagarjuna College of Engineering and technology Bangalore, Karnataka. He received his BE degree in Electronics and Communication from RYMEC, Bellary Visvesvaraya Technological University in 2012, M Tech degree in Digital Communication and Networking from Dr. Ambedkar Institute of technology, Bangalore, in 2015. His research includes Design, Characterization and Optimization of RF Passive Devices, Board Level Tuning and Optimization of Matching Networks, Low Noise Amplifier, Power Amplifier, Circuit Linearization and High-Efficiency Design Techniques and Antenna design.

---